Identification of a mammalian glycerol-3-phosphate phosphatase: Role in metabolism and signaling in pancreatic β-cells and hepatocytes

Yves Mugabo[a,1], Shangang Zhao[a,1], Annegrit Seifried[b], Sari Gezzar[a], Anfal Al-Mass[c,d], Dongwei Zhang[a,2], Julien Lamontagne[a], Camille Attane[a], Pegah Poursharifi[a], José Iglesias[a,3], Erik Joly[a], Marie-Line Peyot[a], Antje Gohla[b], S. R. Murthy Madiraju[a,4], and Marc Prentki[a,4]

[a]Departments of Nutrition and Biochemistry and Montreal Diabetes Research Center, Centre de Recherche du Centre Hospitalier de l'Université de Montréal, Montréal, QC H1W 4A4, Canada; [b]Institute for Pharmacology and Toxicology and Rudolf Virchow Center for Experimental Biomedicine, University of Würzburg, Würzburg 97080, Germany; [c]Montreal Diabetes Research Center, Centre de Recherche du Centre Hospitalier de l'Université de Montréal, Montréal, QC H1W 4A4, Canada; and [d]Department of Experimental Medicine, McGill University, Montréal, QC H3A 0G1, Canada

Edited by John H. Exton, Vanderbilt University School of Medicine, Nashville, TN, and approved December 11, 2015 (received for review July 21, 2015)

Obesity, and the associated disturbed glycerolipid/fatty acid (GL/FA) cycle, contribute to insulin resistance, islet β-cell failure, and type 2 diabetes. Flux through the GL/FA cycle is regulated by the availability of glycerol-3-phosphate (Gro3P) and fatty acyl-CoA. We describe here a mammalian Gro3P phosphatase (G3PP), which was not known to exist in mammalian cells, that can directly hydrolyze Gro3P to glycerol. We identified that mammalian phosphoglycolate phosphatase, with an uncertain function, acts in fact as a G3PP. We found that G3PP, by controlling Gro3P levels, regulates glycolysis and glucose oxidation, cellular redox and ATP production, gluconeogenesis, glycerolipid synthesis, and fatty acid oxidation in pancreatic islet β-cells and hepatocytes, and that glucose stimulated insulin secretion and the response to metabolic stress, e.g., glucolipotoxicity, in β-cells. In vivo overexpression of G3PP in rat liver lowers body weight gain and hepatic glucose production from glycerol and elevates plasma HDL levels. G3PP is expressed at various levels in different tissues, and its expression varies according to the nutritional state in some tissues. As Gro3P lies at the crossroads of glucose, lipid, and energy metabolism, control of its availability by G3PP adds a key level of metabolic regulation in mammalian cells, and G3PP offers a potential target for type 2 diabetes and cardiometabolic disorders.

glycerol-3-phosphate phosphatase | gluconeogenesis | glucolipotoxicity | type 2 diabetes | glucose-stimulated insulin secretion

The glycerolipid/fatty acid (GL/FA) cycle, which is central to energy homeostasis, balances glucose and lipid metabolism (1, 2), and generates metabolic signals (3, 4). This cycle is deregulated in obesity and type 2 diabetes. Under conditions of fuel surfeit with excessive glucose and free fatty acid (FFA) supply, a substantial portion of glucose is used in mammalian cells via formation of glycerol-3-phosphate (Gro3P) and its incorporation into GL via GL/FA cycle (4, 5). The cycle consists of lipogenesis and lipolysis segments and generates intermediates for the synthesis of various types of complex lipids, but also signals that control many biological processes, including insulin secretion and action (3, 6, 7). The proper operation of this cycle possibly protects β-cells and other cell types from glucolipotoxicity and metabolic stress (4, 8, 9).

Lipogenesis, i.e., the successive esterification of glycolysis-derived Gro3P with fatty acyl-CoA (FA-CoA), produces triglyceride (TG), which can be stored as lipid droplets (10). Lipolysis of TG is initiated by adipose TG lipase to generate diacylglycerol (DAG), which is hydrolyzed by hormone sensitive lipase to give rise to monoacylglycerol (MAG). MAG hydrolysis by classical MAG lipase or by α/β-hydrolase domain-6 (ABHD6) to glycerol and FFA completes the lipolytic segment of the GL/FA cycle (2, 3).

Presently glycerol release from mammalian cells is thought to occur exclusively from the lipolytic segment of the GL/FA cycle, and glycerol production is considered to reflect lipolysis flux. We proposed earlier that, at high glucose concentrations, the release of glycerol by β-cells, which do not express glycerokinase that transforms glycerol to Gro3P (4), is a mechanism of "glucolipotoxicity," and that this process is dependent on the lipolysis segment of GL/FA cycle (3, 4). Indeed, mammalian cells are not known to harbor a Gro3P phosphatase (G3PP) (11), which could directly generate glycerol from Gro3P. In an earlier study on mass isotopomer distribution analysis of glucose labeling from [^{13}C]glycerol in the liver, Gro3P hydrolysis activity was speculated but was not directly demonstrated (12). Thus, the fate of Gro3P in mammalian cells is thought to be its conversion to dihydroxyacetone phosphate (DHAP) or lysophosphatidate, the first intermediate of the lipogenic arm of the cycle. However, many microbes (13–15) and plants (16) harbor a G3PP. We now describe that a previously known phosphoglycolate phosphatase (PGP) (17) with an uncertain function in mammalian cells acts as a specific G3PP and plays a pivotal role in the regulation of glucose and lipid metabolism and signaling, as well as in the response to metabolic stress.

Significance

Glycerol-3-phosphate (Gro3P) lies at the crossroads of glucose, lipid, and energy metabolism in mammalian cells and is thought to participate in glycolysis or in gluconeogenesis, lipid synthesis, and Gro3P electron transfer shuttle to mitochondria. We now report a previously unidentified pathway of Gro3P metabolism in mammalian cells with the identification of Gro3P phosphatase (G3PP) that can directly hydrolyze Gro3P to glycerol. We observed that G3PP expression level controls glycolysis, lipogenesis, lipolysis, fatty acid oxidation, cellular redox, and mitochondrial energy metabolism in β-cells and hepatocytes, as well as glucose-induced insulin secretion and the response to metabolic stress in β-cells, and in gluconeogenesis in hepatocytes. G3PP is a previously unknown player in metabolic regulation and signaling and offers a potential target for cardiometabolic disorders.

Author contributions: S.R.M.M. and M.P. designed research; Y.M., S.Z., A.S., S.G., A.A.-M., D.Z., J.L., C.A., P.P., J.I., S.R.M.M., and M.P. performed research; A.S. and A.G. contributed new reagents/analytic tools; Y.M., E.J., M.-L.P., S.R.M.M., and M.P. analyzed data; and Y.M., S.R.M.M., and M.P. wrote the paper.

The authors declare no conflict of interest.

This article is a PNAS Direct Submission.

[1]Y.M. and S.Z. contributed equally to this work.

[2]Present address: Diabetes Research Center, Beijing University of Chinese Medicine, Beijing 100029, China.

[3]Present address: Departamento de Nutricion y Bioquímica, Pontificia Universidad Javeriana, Cra 7, No 43-82, Edf. Carlos Ortiz, Bogotá, Colombia.

[4]To whom correspondence may be addressed. Email: murthy.madiraju@crchum.qc.ca or marc.prentki@umontreal.ca.

This article contains supporting information online at www.pnas.org/lookup/suppl/doi:10.1073/pnas.1514375113/-/DCSupplemental.

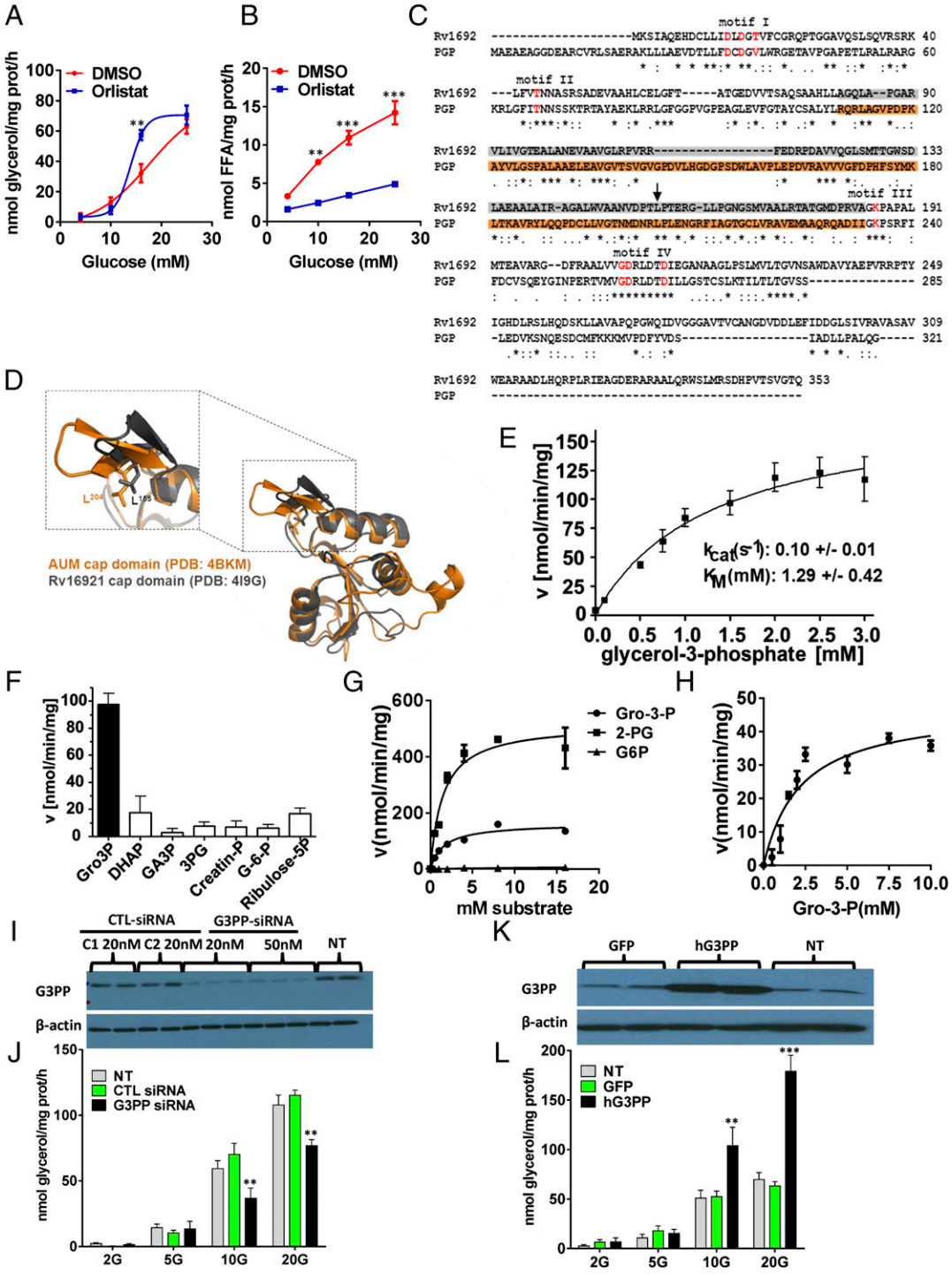

Fig. 1. Identification of PGP as a G3PP and its effect on glycerol release in rat islet cells and INS832/13 β cells. (*A* and *B*) Glycerol and FFA release (2 h) by isolated rat islets at 4, 10, 16, and 25 mM glucose with and without 50 μM orlistat (means ± SEM of four independent experiments with triplicate observations; $^{**}P < 0.01$ and $^{***}P < 0.001$). (*C* and *D*) Alignment of murine PGP (mPGP) and G3PP of *Mycobacterium tuberculosis* (*Rv1692*). (*C*) There is a very high degree of sequence homology ($P < 4 \times 10^{-20}$) and all active-site residues (in red) match exactly. (*D*) The cap-domains, which determine substrate specificity (in orange for mPGP and gray for Rv1692) align nearly perfectly, as does the critical leucine residue at position 204 in PGP and 155 in Rv1692 (*C*, black arrow). (*E*) Kinetics of Gro3P hydrolysis by purified mPGP (mean ± SEM from eight experiments). (*F*) Purified mPGP hydrolyzes Gro3P more effectively than related compounds (mean ± SEM of five experiments). creatine-P, creatine phosphate; G-6-P, glucose-6-phosphate; GA3P, D,L-glyceraldehyde-3-phosphate; 3PG, D(-)3-phosphoglycerate; ribose-5P, ribulose-5-phosphate. (*G*) Kinetics of Gro3P, 2-PG, and glucose-6-phosphate (G-6-P) hydrolysis by overexpressed human G3PP in 293T cell extracts (mean ± SEM; $n = 4$). (*H*) Kinetics of Gro3P hydrolysis by native rat G3PP in INS832/13 cell extracts (mean ± SEM; $n = 4$). (*I* and *J*) RNAi knockdown of PGP/ G3PP in INS832/13 cells reduces glucose-induced glycerol release. (*I*) PGP/G3PP protein expression 48 h after transfection with 20 nM and 50 nM G3Pase siRNA or control siRNA C1 and C2 or in nontransfected (NT) cells. (*J*) Glycerol release (2 h) with and without RNAi knockdown at 2, 5, 10, and 20 mM glucose [mean ± SEM; $n = 4$; $^{**}P < 0.01$ vs. control (CTL) cells]. (*K* and *L*) Overexpression of hG3Pase in INS832/13 cells enhances glucose-induced glycerol release. (*K*) hPGP/G3PP protein expression after transfection with GFP and G3PP expression plasmids and in nontransfected cells. (*L*) Glycerol release at 2, 5, 10, and 20 mM glucose (mean ± SEM; $n = 4$; $^{**}P < 0.01$ and $^{***}P < 0.001$ vs. GFP control cells).

Results and Discussion

Dichotomy in Orlistat Effect on Glycerol and FFA Release in β-Cells. The discovery of a mammalian G3PP started from the fortuitous observation of a dichotomy of inhibitory effects of the panlipase and lipolysis inhibitor orlistat on glycerol and FFA release at various glucose concentrations from β-cells. Thus, orlistat inhibited lipolysis at high glucose concentrations in INS832/13 β-cells and in rat islets as evidenced by the reduction in FFA release; however, the increased release of glycerol in the presence of elevated glucose concentration was not inhibited (Fig. 1 *A* and *B* and Fig. S1 *A* and *B*), indicating that not all glucose-derived glycerol arises from lipolysis. In rat islet cells, at medium concentration of glucose (10 mM), orlistat showed moderate inhibition of glycerol release, indicating that, at this glucose concentration, a small amount of glycerol does arise from lipolysis. Thus, in β-cells, there must exist an alternate mechanism for the production of glycerol besides lipolysis. The direct hydrolysis of glucose-derived Gro3P by a hypothetical G3PP is a plausible source of glycerol.

Structural Similarity Between PGP and Bacterial G3PP. A BLAST analysis of various known G3PP enzymes against mammalian sequences led to the identification of PGP (17), whose function in mammalian cells is uncertain and which belongs to the class of haloacid dehalogenase (HAD)-type hydrolases. Recently PGP was suggested to possess protein tyrosine phosphatase activity and was called "aspartate-based, ubiquitous, Mg^{2+}-dependent phosphatase" (AUM) (18). Although the catalytic efficiency of AUM/PGP toward the generic protein tyrosine phosphatase substrate *p*-nitrophenolphosphate was ∼1,000-fold higher than the activity of the well-established HAD-type protein tyrosine phosphatase Eya3, its activity was ∼1,000-fold less than that of classical tyrosine phosphatases like PTP1B, TCPTP, or SHP1, raising the possibility that PGP/AUM may also dephosphorylate other low molecular weight substrates/metabolites in addition to those reported previously (18). An amino acid sequence comparison and structural overlay showed high similarity of the murine PGP/AUM cap with the cap domain of the recently described mycobacterial G3PP, Rv1692 (13), in residue orientation and composition, and suggested that PGP is indeed a bona fide G3PP (Fig. 1 *C* and *D* and Fig. S1*C*). PGP belongs to the subtype of cap-domain containing HAD-phosphatases. This domain features a specificity loop with evolutionarily highly conserved residues that are required for proper substrate coordination in the active site of the hydrolase (19, 20). The sequence alignment of Rv1692 and mPGP revealed conservation of a number of those amino acid residues that were recently identified to be important for proper substrate positioning in murine PGP/AUM (18). There is near-perfect alignment of the cap domains of PGP and Rv1692 and of the critical leucine residue at positions 204 in mPGP (18) and 155 in Rv1692, as revealed by structural overlay (Fig. 1*D*). A zoom in the substrate binding pocket shows that the critical and evolutionarily conserved cap domain residues involved in substrate coordination are identical between PGP and the mycobacterial G3PP, Rv1692 (Fig. S1*C*).

PGP Acts as a Specific G3PP. Purified recombinant murine PGP, expressed as described before (18), showed activity with Gro3P, with a K_m of 1.29 mM and k_{cat} of 0.1 s^{-1} (Fig. 1*E*). At saturating substrate concentration, mPGP showed specific activity of ∼100 nmol/min/mg protein with Gro3P, whereas its activity toward other related substrates such as DHAP, glyceraldehyde-3-phosphate, 3-phosphoglycerate, creatine phosphate, glucose-6-phosphate, and ribulose-5-phosphate was much lower (Fig. 1*F*). Activity with inositol 3,4,5-trisphosphate and lysophosphatidic acid was seen only with very high nonphysiological concentrations of these compounds. The overexpressed human PGP in 293T cell extracts showed similar K_m (∼1.4 mM) for Gro3P as the purified murine PGP and a V_{max} of ∼150 nmol/min/mg protein (Fig. 1*G*). Human PGP in whole-cell extracts showed similar affinity for 2-phosphoglycolate (2-PG; ∼1.5 mM) but higher V_{max} (∼500 nmol/min/mg protein), indicating that this enzyme has higher capacity to hydrolyze 2-PG (Fig. 1*G*). Under the same incubation conditions, activity with glucose-6-phosphate was negligible (Fig. 1*G*). In INS832/13 rat β-cells, there was a significant amount of native PGP/G3PP enzyme in terms of V_{max}, which was 47 nmol/min/mg protein (Fig. 1*H*). High glucose concentration stimulated glycerol release in INS832/13 β-cells was reduced by RNAi knockdown of native PGP (Fig. 1 *I* and *J* and Fig. S1*D*), greatly elevated by overexpression of human PGP (Fig. 1 *K* and *L*), and the decrease caused by RNAi knockdown was reversed by overexpression of hPGP in the same cells (Fig. S1*E*). Overall, the data demonstrate that PGP acts as a G3PP in vitro and in intact cells.

G3PP Activity Controls Insulin Secretion and Glucolipotoxicity in Pancreatic β-Cells. As Gro3P is one of the starting substrates for the GL/FA cycle that produces lipid signals for glucose-stimulated insulin secretion (GSIS), alteration of Gro3P levels by G3PP should influence insulin secretion (21). All three different G3PP-siRNAs reduced G3PP expression effectively (Fig. S1*D*), and we selected G3PP-siRNA-1 and control siRNA-1 for rest of the study. In accordance with this prediction, RNAi knockdown of native rat G3PP in INS832/13 β-cells elevated GSIS (Fig. 2*A*), whereas overexpression of hG3PP reduced GSIS (Fig. 2*B*) without affecting basal secretion. Similar results were obtained in isolated rat islets infected with lentiviral shRNA-G3PP for RNAi knockdown or adenoviral hG3PP for overexpression (Fig. 2 *C* and *D*). The role of G3PP activity in regulating GSIS was confirmed by the observation that overexpression of hG3PP in INS832/13 cells curtailed the increased GSIS caused by RNAi knockdown of endogenous G3PP (Fig. S1*F*).

Chronic elevated glucose exposure of β-cells without or with high concentrations of exogenous FFA cause glucotoxicity and glucolipotoxicity, respectively, as indicated by caspase-3 activity, an index of apoptosis (22). The mechanism involves enhanced glucose metabolism and esterification of FFA (23), resulting in mitochondrial dysfunction, reactive oxygen species (ROS) production, and endoplasmic reticulum (ER) stress. Reducing G3PP expression in INS832/13 β-cells, which is likely to elevate the formation of glycerolipid intermediates, caused enhanced glucotoxicity (Fig. 2*E*), whereas overexpression of hG3PP led to decreased glucotoxicity (Fig. 2*F*). Glucolipotoxicity, which was enhanced by G3PP knockdown, was curtailed by hG3PP overexpression that also reversed the toxic effect of G3PP knockdown under glucolipotoxic condition (Fig. 2*G*). Thus, changes in G3PP activity in the β-cell modulate insulin secretion and the response to metabolic stress.

Tissue Distribution and Nutritional Regulation of G3PP. Expression of G3PP at the mRNA (Fig. S2 *A*, *C*, and *E*) and protein (Fig. S2 *B*, *D*, and *F*) levels is apparently ubiquitous, as it was detected in all tissues examined; it was found to be particularly high in testis, followed by heart, skeletal muscle, and islet tissue. Liver, kidney, intestine, and visceral white adipose tissue showed low expression, probably because these tissues are engaged in gluconeogenesis and/or lipogenesis, both of which require Gro3P supply. The high expression of G3PP in heart and skeletal muscle possibly ensures no toxic accumulation of lipids in these fat-burning tissues (24). The role of this enzyme in testis is not clear.

G3PP expression is regulated by nutritional status. Thus, G3PP mRNA and protein is inversely changed in white adipose vs. brown adipose tissue (BAT) under fed and fasted states (Fig. S2 *A* and *B*) and under high-fat diet (HFD) vs. normal diet conditions (Fig. S2 *C* and *D*). These changes may reflect the adaptation for regulation of nutrient metabolism in adipose tissues. Thus, elevated G3PP in white adipose tissue in fasted state ensures supply of glycerol into circulation rather than glycerol reincorporation

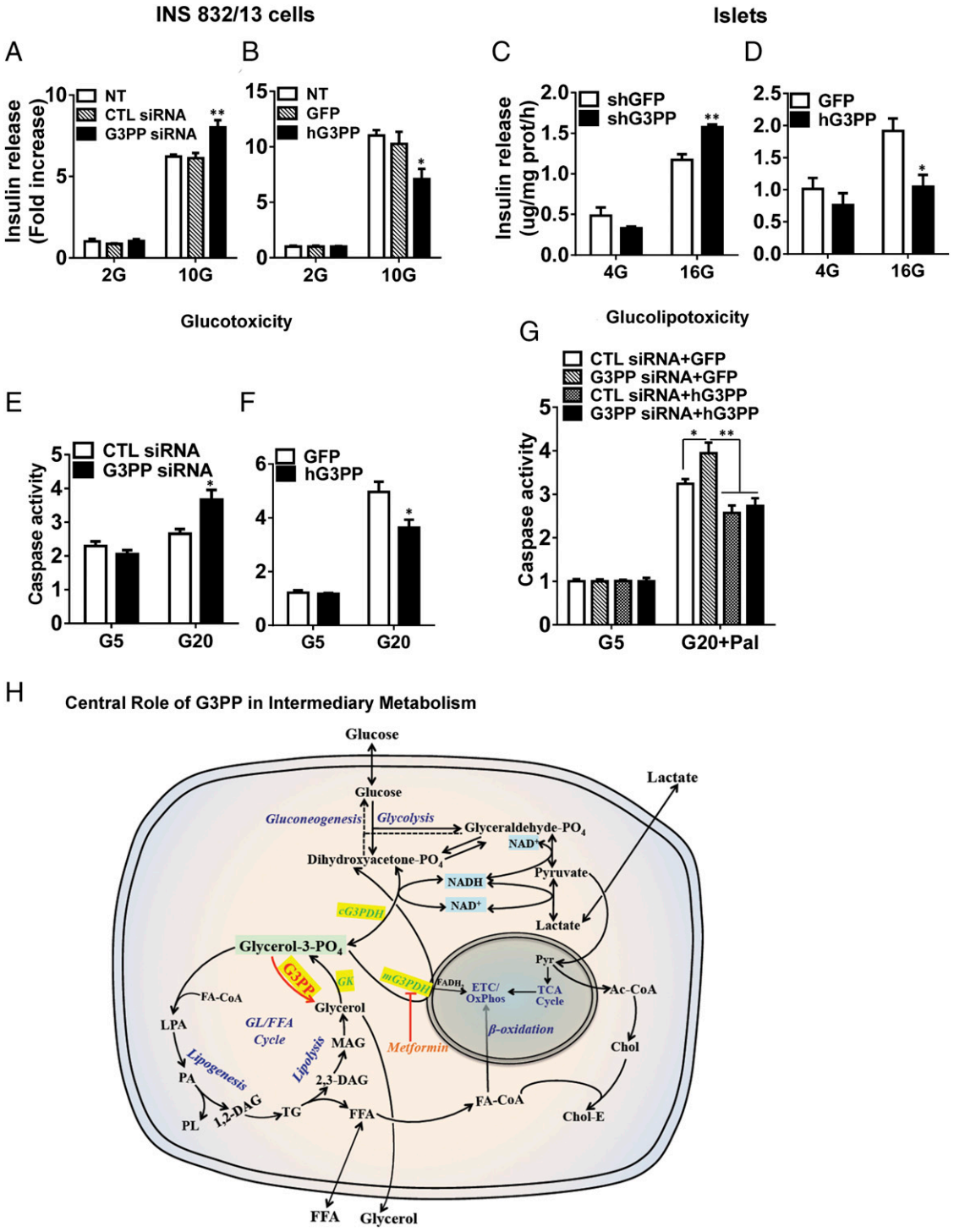

Fig. 2. Activity of G3PP controls GSIS, glucotoxicity, and glucolipotoxicity in β-cells. (*A* and *B*) Insulin secretion in INS832/13 cells at 2 mM and 10 mM glucose after G3PP knockdown (*A*) or hG3PP overexpression (*B*). CTL, control; NT, not transfected (mean ± SEM of three experiments with triplicate observations; $*P < 0.05$ and $**P < 0.01$ vs. corresponding controls). (*C* and *D*) Insulin secretion in isolated rat islet cells at 4 mM and 16 mM glucose after G3PP knockdown (*C*) or hG3PP overexpression (*D*) (mean ± SEM of three experiments with triplicate observations; $*P < 0.05$ and $**P < 0.01$ vs. corresponding controls). (*E* and *F*) Glucose-induced apoptosis (glucotoxicity) in INS832/13 cells after G3PP knockdown for 24 h (*E*) or hG3PP overexpression for 72 h (*F*). Caspase activity was determined in cells exposed to 5 mM and 20 mM glucose (mean ± SEM of three experiments with triplicate observations; $*P < 0.05$ vs. corresponding controls). (*G*) Glucose plus palmitate-induced apoptosis (glucolipotoxicity) in INS832/13 cells after G3PP RNAi knockdown with or without rescue by hG3PP overexpression. Controls were set up with control siRNA for knockdown and GFP for overexpression. Glucolipotoxicity was induced for 48 h by 20 mM glucose plus 0.3 mM palmitate and compared with 5 mM glucose value (mean ± SEM of three experiments with triplicate observations; $*P < 0.05$ and $**P < 0.01$ vs. corresponding controls; control siRNA, shG3PP, and GFP). (*H*) Scheme illustrating the central role of G3PP in intermediary metabolism. Gro3P formed from glucose metabolism or by the phosphorylation of lipolysis-derived glycerol is at the crossroads of intermediary metabolism. G3PP, by controlling Gro3P, plays a central role in the regulation of intermediary and energy metabolism and cellular redox. Ac-CoA, acetyl-CoA; cG3PDH, cytosolic G3PDH; Chol, free cholesterol; Chol-E, cholesterol ester; ETC, electron transport chain; FA-CoA, fatty acyl-CoA; GK, glycerokinase; GL/FFA, glycerolipid/FFA; LPA, lysophosphatidic acid; mG3PDH, mitochondrial G3PDH; OxPhos, oxidative phosphorylation; PA, phosphatidic acid; PL, phospholipids; Pyr, pyruvate.

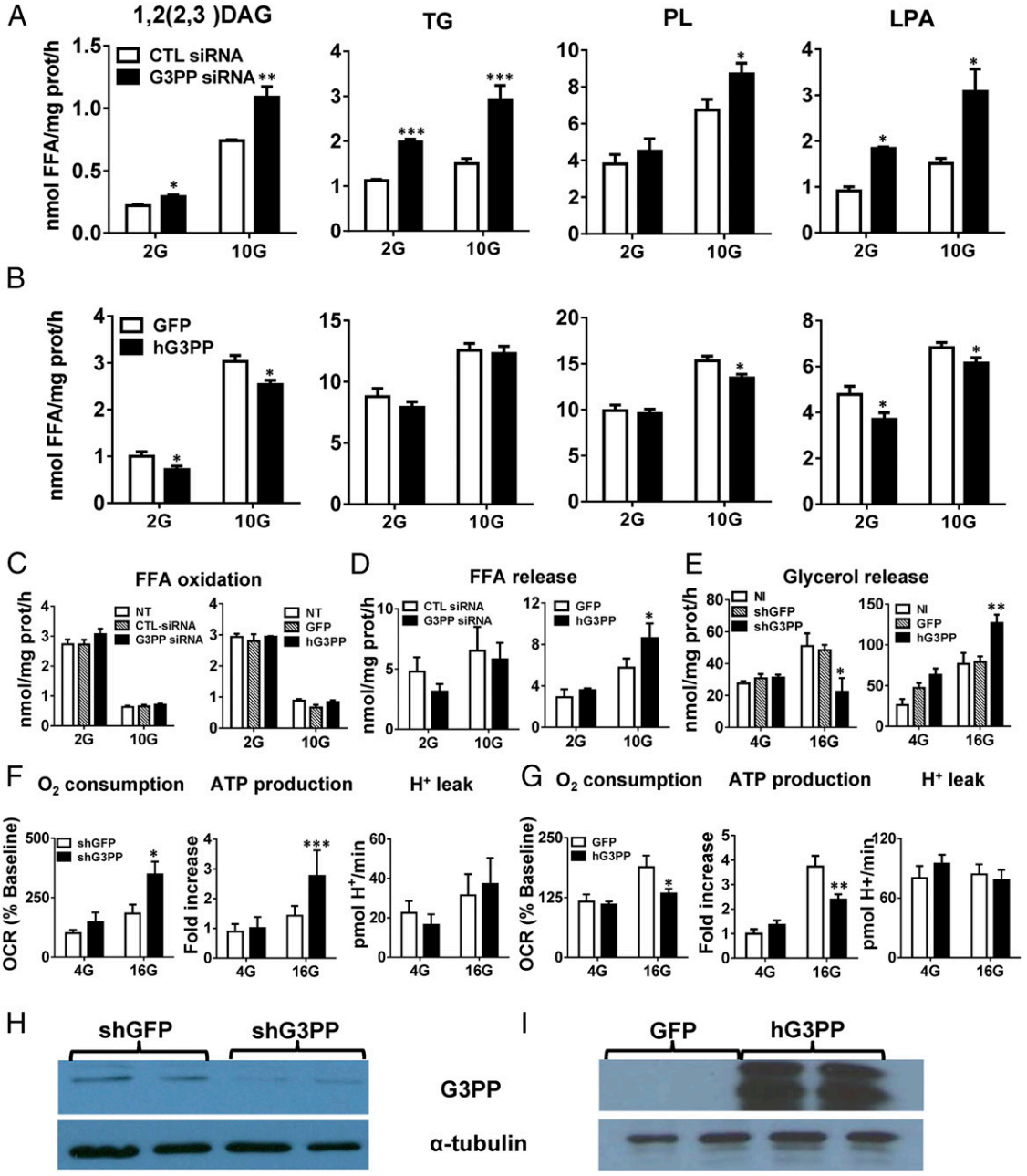

Fig. 3. Changes in G3PP expression modulate glucose, lipid, and energy metabolism in β-cells. (*A* and *B*) Effect on fatty acid esterification at 2 mM and 10 mM glucose. (*A*) RNAi knockdown of G3PP and (*B*) overexpression of hG3PP in INS832/13 cells. LPA, lysophosphatidic acid; PL, phospholipids. siRNA and GFP controls are indicated (mean ± SEM; $n = 9$; *$P < 0.05$, **$P < 0.01$, and ***$P < 0.001$). (*C*) Palmitate oxidation in INS832/13 cells at 2 mM and 10 mM glucose. NT, not transfected (mean ± SEM; $n = 6$). (*D*) FFA release from INS832/13 cells at 2 mM and 10 mM glucose (mean ± SEM; $n = 6$; *$P < 0.05$). (*E*) Glycerol release from rat islet cells at 4 mM and 16 mM glucose following RNAi knockdown of G3PP with lentiviral-shG3PP or hG3PP overexpression with adenoviral-hG3PP. NI, not infected (mean ± SEM; $n = 9$; *$P < 0.05$ and **$P < 0.01$). (*F* and *G*) Respiration and mitochondrial function in rat islets at 4 mM and 16 mM glucose following RNAi knockdown of G3PP (*F*) or hG3PP overexpression (*G*) (mean ± SEM; $n = 9$; *$P < 0.05$, **$P < 0.01$, and ***$P < 0.001$). (*H* and *I*) Western blot analysis of G3PP protein in rat islets after RNAi knockdown (*H*) or overexpression of hG3PP (*I*).

into glycerolipids (25) for the purposes of gluconeogenesis in liver and kidney, whereas the decreased G3PP expression in BAT ensures trapping of incoming FFA and glucose into glycerolipids for future use, as well as for fuel use for thermogenesis during fasting. Conversely, the decreased expression of G3PP in white adipose tissue in HFD condition should help in the storage of fat, whereas, in BAT, such storage is not needed and the elevated G3PP levels ensure effective burning of fatty acids in BAT mitochondria. Hence, nutritional control of G3PP exemplifies the importance of this enzyme in fuel and energy metabolism as its expression is differentially regulated in different tissues.

G3PP Expression Level Influences Glucose, Lipid, and Energy Metabolism in β-Cells. Because Gro3P is a central metabolic intermediate that lies at the crossroads of glucose and lipid metabolism, we examined whether G3PP also plays a critical role in metabolic regulation (Fig. 2*H*). As expected, RNAi knockdown of G3PP in INS832/13 cells increased the synthesis of 1,2(2,3)-DAG, 1,3-DAG, TG, total phospholipids, lysophosphatidylinositol,

lysophosphatidate, and lysophosphatidylcholine (Fig. 3*A* and Fig. S3*A*), whereas overexpression led to their decreased synthesis (Fig. 3*B* and Fig. S3*B*). Considering that many of these lipids have signaling roles in different cells (3), G3PP is likely to regulate these signaling pathways. In INS832/13 cells, altered activity of G3PP had no effect on fatty acid oxidation at low or high glucose concentration (Fig. 3*C*). FFA release from these cells, which is mostly dependent on lipolysis, was elevated when G3PP was overexpressed, indicating that a reduction in Gro3P levels following G3PP overexpression lowers the reesterification of FFA, leading to their elevated release from the cells (Fig. 3*D*). In rat islets, glucose-stimulated glycerol release was lowered by G3PP knockdown and increased by G3PP overexpression (Fig. 3*E*), similar to that noticed with INS832/13 cells (Fig. 1 *J* and *L*).

As Gro3P directly transfers electrons to mitochondria via the action of mitochondrial Gro3P dehydrogenase, changes in Gro3P levels during glucose oxidation are expected to influence respiration. Thus, in rat islet cells, reducing G3PP expression led to elevated O_2 consumption and ATP production (Fig. 3*F*), whereas hG3PP overexpression caused opposite changes (Fig. 3*G*), without affecting H^+ leak in both cases. Similar results were obtained by using INS832/13 cells (Fig. S3 *C* and *D*). Altered G3PP protein levels were confirmed in rat islet cells after shRNA knockdown and hG3PP overexpression (Fig. 3 *H* and *I*). The increased ATP levels in β-cells by G3PP knockdown relate to the increased GSIS seen under these conditions (21). Thus, altered expression of G3PP in β-cells has a significant impact on glucose, lipid, and mitochondrial metabolism, and consequently on the response of these cells for metabolic signal transduction and GSIS.

G3PP Controls Glycolysis, Gluconeogenesis, and Lipid Metabolism in Hepatocytes. Liver is the major site of gluconeogenesis starting from amino acids or adipose lipolysis-derived glycerol, and both pathways involve the formation of Gro3P (Fig. 2*H*). Thus, in primary rat hepatocytes, shRNA knockdown of G3PP (Fig. S4*A*) led to a great increase in gluconeogenesis from glycerol and from pyruvate plus lactate (Fig. 4*A*), whereas overexpression of hG3PP in these cells (Fig. S4*B*) completely curtailed gluconeogenesis (Fig. 4*F*).

Fatty acid oxidation in liver is dependent on the availability of fatty acyl-CoA substrate, which is controlled by the extent of esterification by glycerol-phosphate acyltransferase-1 (26). Fatty acid oxidation was directly related to G3PP expression levels in rat hepatocytes, and, at high glucose levels, which suppress β-oxidation, elevated G3PP expression led to enhanced fatty acid oxidation (Fig. 4 *B* and *G*). This is different from the results with INS832/13 cells and probably reflects the highly lipogenic nature of liver tissue compared with β-cells. Thus, FFA entering cells must be esterified before being oxidized following lipolysis of endogenous lipid stores (27). In hepatocytes as well, glycerol release at high glucose levels was reduced by G3PP knockdown and elevated by its overexpression (Fig. 4 *C* and *H*).

Knockdown of G3PP in hepatocytes enhanced lactate production and release, an index of glycolytic flux, as expected, because of decreased diversion of glucose carbons in the form of glycerol via G3PP (Fig. 4 *D* and *E*). Conversely, overexpression of hG3PP had the reverse effects, reducing glycolytic flux (Fig. 4 *I* and *J*). The overall increase in glycolytic flux compared with noninfected cells is a result of viral infection, which is known to accelerate glycolysis (28, 29). Similar to the changes in INS832/13 cells, lipogenesis was affected by altered G3PP expression in rat hepatocytes (Fig. 4 *K* and *L* and Fig. S4 *C* and *D*). Formation of cholesterol esters was markedly decreased by the overexpression of G3PP in liver cells (Fig. S4*D*), and this may be a result of reduced availability of fatty acyl groups because of their enhanced flux through mitochondrial β-oxidation.

Regulation of Cellular Redox and Energy Production by G3PP. Metabolite measurements using LC-MS/MS (liquid chromatography/tandem mass spectroscopy) in rat hepatocytes revealed a significant decrease in Gro3P and DHAP following hG3PP overexpression, whereas G3PP knockdown led to a marked increase in Gro3P at 25 mM glucose (Fig. 5 *A* and *B*). We calculated the intracellular metabolite concentrations assuming average intracellular water volume to be 2.54 μL/mg protein (30). Intracellular Gro3P concentrations in control hepatocytes were 2 mM and 4.5 mM at 5 mM and 25 mM glucose, respectively, and the corresponding DHAP concentrations were 0.03 mM and 0.095 mM, respectively. Thus, the intracellular Gro3P concentration is sufficient for the G3PP to use this substrate effectively, as it is in the range of its K_m value. The ratio of Gro3P/DHAP increased greatly only when G3PP was knocked down at 25 mM glucose (Fig. 5*C*). Lactate levels decreased and pyruvate levels increased after G3PP overexpression, and the opposite changes were noted after G3PP knockdown (Fig. 5 *D* and *E*). This is in line with the enzymatic measurements of

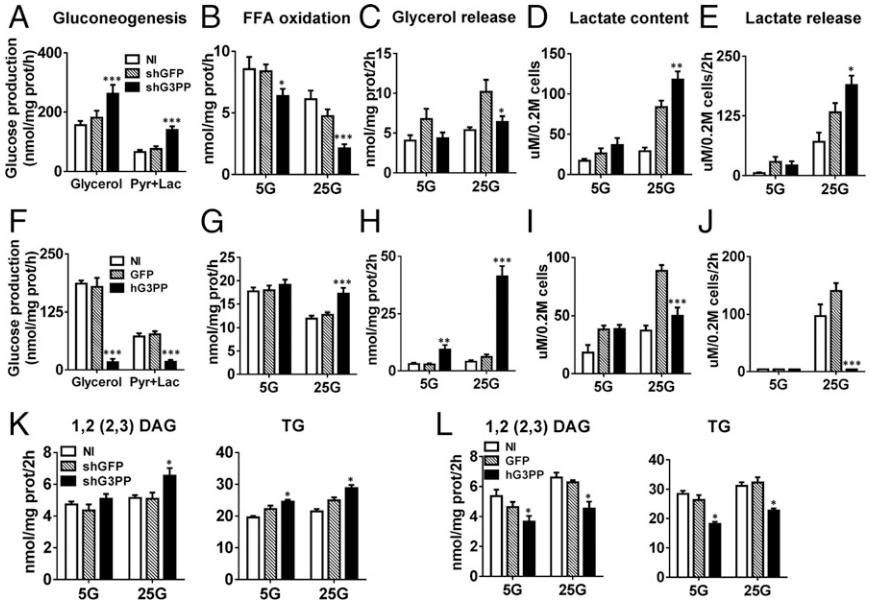

Fig. 4. Effect of altered G3PP expression on liver metabolism in vitro. (*A*–*L*) In vitro metabolic experiments with rat primary hepatocytes infected with lentivirus-shG3PP and control lentivirus-shGFP for G3PP knockdown (*A*–*E*) or with adenovirus-hG3PP and control adenovirus-GFP for overexpression of hG3PP (*F*–*J*) (mean ± SEM; $n = 6$–8; $^*P < 0.05$, $^{**}P < 0.01$, and $^{***}P < 0.001$ vs. shGFP or GFP controls). (*A* and *F*) Gluconeogenesis from glycerol or pyruvate/lactate; (*B* and *G*) palmitate oxidation at 5 mM and 25 mM glucose (5G and 25G); (*C* and *H*) glycerol release; (*D* and *I*) lactate production (intracellular content); (*E* and *J*) lactate release; and (*K* and *L*) fatty acid esterification using [1-^{14}C]palmitate. 1,2(2,3)-DAG and TG synthesis in hepatocytes with G3PP knockdown (*K*) or with hG3PP overexpression (*L*).

lactate (Fig. 4 *D*, *E*, *I*, and *J*). Interestingly, the ratio of lactate to pyruvate, which reflects the cytosolic redox, was decreased by G3PP overexpression and increased by G3PP knockdown (Fig. 5*F*), indicating that G3PP regulates cellular redox. Thus, G3PP levels were reciprocally related to cellular total NADH levels (Fig. 5*G*). We also noticed a significant decline in total NAD^+ levels by G3PP overexpression (Fig. 5*H*), which may be related to lowered production of ATP (Fig. 5*K*), which is needed for the synthesis of NAD^+. Such reduced formation of ATP during respiration was also observed in rat islet cells (Fig. 3*G*). Changes in cellular redox ratio (i.e., NADH/NAD^+) were more evident upon G3PP knockdown than after G3PP overexpression (Fig. 5*I*), probably because of reduced total NAD^+ levels. These results suggest that G3PP, by promoting Gro3P to glycerol conversion, actually regulates NADH/NAD^+ ratio in the cell and thus ATP production. Thus, overexpression of G3PP causes a shift in glucose carbon flux toward glycerol formation, leading to a decrease in DHAP and also in NADH (used for DHAP-to-Gro3P conversion; see Fig. 2*H*), which results in reduced ATP formation and also reduced lactate production, an index of glycolysis, in hepatocytes. The reverse is true when G3PP is knocked down, leading to elevated ATP production. Thus, G3PP appears to directly regulate cellular redox and energy production.

Gro3P but Not 2-Phosphoglycolate Is the Physiologically Relevant Substrate for G3PP/PGP. Significantly, 2-PG levels were found to be very low (<0.04 nmol/mg protein or <0.02 mM), approximately 250-fold lower than Gro3P levels and also ∼75-fold lower than the K_m for PGP/G3PP, in hepatocytes, and the cellular content of G3PP/PGP had no major effect on 2-PG levels (Fig. 5*J*). However, Gro3P cellular concentration calculated from our results on hepatocytes ranges from 2 mM to 4.5 mM at low and high glucose concentrations. Similarly, in INS832/13 cells, Gro3P concentration was calculated to be ∼1.5 mM at 10 mM glucose concentration (31). These cellular concentrations of Gro3P are quite favorable for G3PP/PGP to use this substrate effectively. Thus, our results indicated that 2-PG is not a physiologically relevant substrate for this enzyme, at least in hepatocytes, even though this enzyme can efficiently hydrolyze 2-PG when available at very high concentrations in a cell extract. It is important to keep in mind that 2-PG is formed in cells during repair of DNA strands when they are broken, for example, in the presence of chemical agents like bleomycin or radiation (32), and its levels in normal tissues and cells are quite low. It has been reported earlier that 2-PG levels in liver tissue are approximately 19–20 μM (33) and that, in many other tissues and blood, this metabolite is present in micromolar concentrations only. Therefore, the normal physiological function of this enzyme is very likely to be in the control of Gro3P levels via its hydrolysis.

In Vivo Overexpression of G3PP Reduces Hepatic Glucose Production and Plasma TGs in Rats. To further understand the metabolic regulatory role of G3PP, we injected adenoviral vector coding for hG3PP (Adv-hG3PP) or GFP (Adv-GFP; control) to rats. One week after injection, expression of G3PP in liver was greatly elevated (Fig. 6 *A* and *B*), whereas it was not altered in other tissues (Fig. S4*G*). One day after injection, Adv-hG3PP–injected rats showed ∼10% reduction in body weight (BW), which was maintained for the next 6 d compared with Adv-GFP–injected rats (Fig. 6 *C* and *D*). Adv-G3PP rats also showed a modest reduction in cumulative food

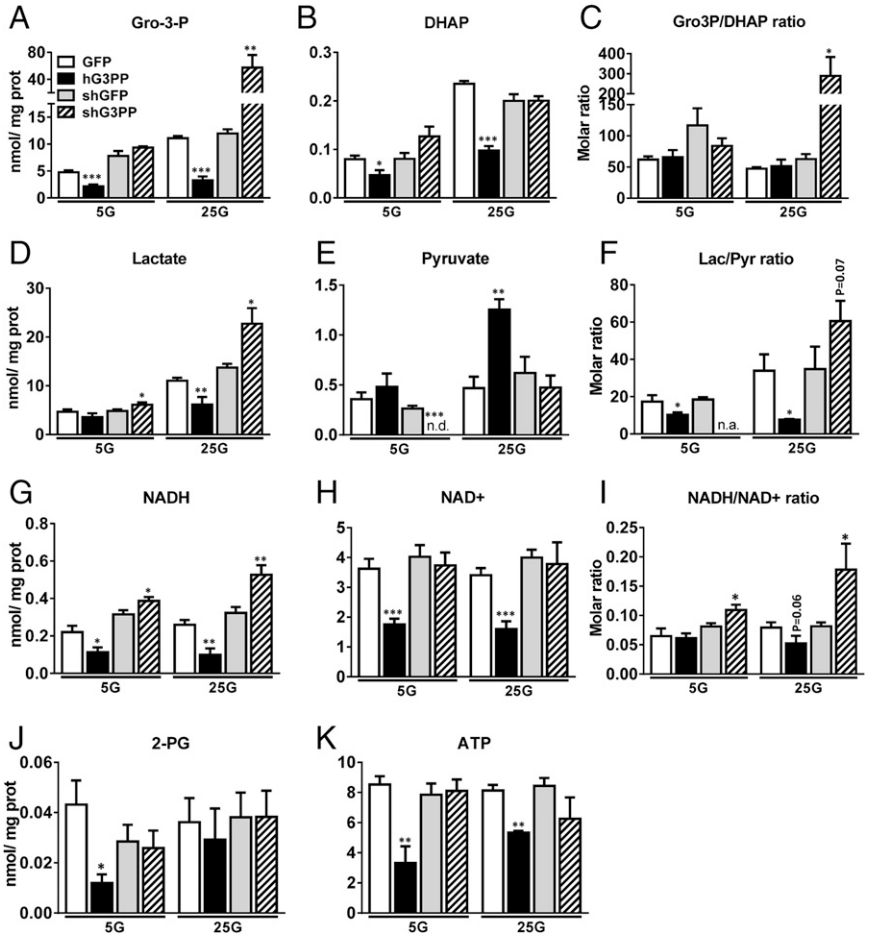

Fig. 5. Effect of altered G3PP expression on metabolite levels in primary rat hepatocytes. (*A*–*K*) Targeted metabolomics of rat primary hepatocytes infected with adenovirus-hG3PP (hG3PP) and control adenovirus-GFP (GFP) for overexpression of hG3PP or with lentivirus-shG3PP (shG3PP) and control lentivirus-shGFP (shGFP) for G3PP knockdown. After infections, hepatocytes were incubated at 5 mM or 25 mM glucose for 2 h. Then, the cells were processed for metabolite measurements as described in *Materials and Methods*. Metabolite content is expressed as nmol/mg protein. (*A*) Gro3P, (*B*) DHAP, (*C*) Gro3P/DHAP ratio; and (*D*) lactate, (*E*) pyruvate, and (*F*) lactate/pyruvate ratio; and (*G*) NADH, (*H*) NAD^+, (*I*) NADH/NAD^+, (*J*) 2-PG, and (*K*) ATP (mean ± SEM; $n = 6$; $^*P < 0.05$, $^{**}P < 0.01$, and $^{***}P < 0.001$ vs. shGFP or GFP controls).

intake (Fig. 6*E*). After one week, plasma glycerol levels were markedly elevated (Fig. 6*F*), indicating that the overexpressed G3PP in liver is able to generate glycerol in vivo, which is released into blood. In agreement with the observation in isolated hepatocytes and INS832/13 cells, in vivo liver overexpression of G3PP led to reduced plasma TG levels (Fig. 6*G*), which is likely a result of reduced hepatic TG synthesis. Circulating LDL and HDL were modestly affected, with HDL showing a significant increase (Fig. S4 *E* and *F*) and LDL showing a decreasing trend. Hepatic glucose production from glycerol during a glycerol load test was reduced in Adv-G3PP–injected rats (Fig. 6*H*), showing that liver gluconeogenesis from glycerol was affected, as was the case with isolated rat hepatocytes.

Conclusion

The possibility of Gro3P hydrolysis in mammalian cells (34) and fish (11, 35) was previously considered, but no clear evidence could be obtained. In a recent work, it has been suggested that, in liver, there is a NADH/NAD$^+$ ratio-dependent direct formation of glycerol from Gro3P, generated by high carbohydrate intake, particularly under conditions of mitochondrial aspartate-glutamate carrier isoform-2 (i.e., citrin) deficiency; however, no enzyme for this conversion was suggested (36).

Recently, it has been proposed that the action of the antidiabetic agent metformin entails, at least in part, mitochondrial Gro3P dehydrogenase (G3PDH) inhibition, resulting in increased hepatic cytosolic redox that lowers hepatic gluconeogenesis (37) (Fig. 2*H*). In the present work, the net anticipated result of enhanced G3PP activity and reduced Gro3P levels is also decreased flux through mitochondrial G3PDH because there is less substrate for this enzyme. However, G3PP activation will result in decreased cytosolic NADH rather than increased, as metformin does. Thus, because of the irreversible nature of G3PP reaction, its overactivity pulls glycolytic carbon flux toward glycerol formation. As a result, cytosolic NADH, which is formed during glycolysis, is consumed to reduce dihydroxyacetone-phosphate to Gro3P by cytosolic Gro3P dehydrogenase. Hence, metformin and elevated G3PP activity inhibit gluconeogenesis, but via different mechanisms: metformin by increasing the cytosolic redox and G3PP by removing Gro3P and dihydroxyacetone-phosphate, the substrates of gluconeogenesis (Fig. 2*H*).

In sum, we have identified a metabolic enzyme in mammalian cells that can directly transform Gro3P to glycerol. The identification of a previously unrecognized G3PP in mammalian cells is an important addition to our understanding of metabolic regulation and signaling at large. We have shown that G3PP expression level controls several metabolic pathways and biological processes (Fig. 2*H*) in a tumoral β-cell line and in normal rat islet cells as well as in hepatocytes. These include, depending on the cell type, glycolysis, gluconeogenesis, lipogenesis, phospholipid synthesis, lipolysis, fatty acid oxidation and mitochondrial energy metabolism, cellular redox, and ATP production. In addition, G3PP regulates glucose-induced insulin secretion and the response to metabolic stress in the β-cell. Thus, G3PP is an attractive target for metabolic syndrome-related disorders. It is anticipated that enhanced activity of G3PP to be beneficial under conditions of type 2 diabetes and obesity, as it protects β-cells from fuel surfeit toxicity and from exhaustion caused by overstimulation by high glucose concentrations and reduces hepatic glucose production and the lipogenic burden.

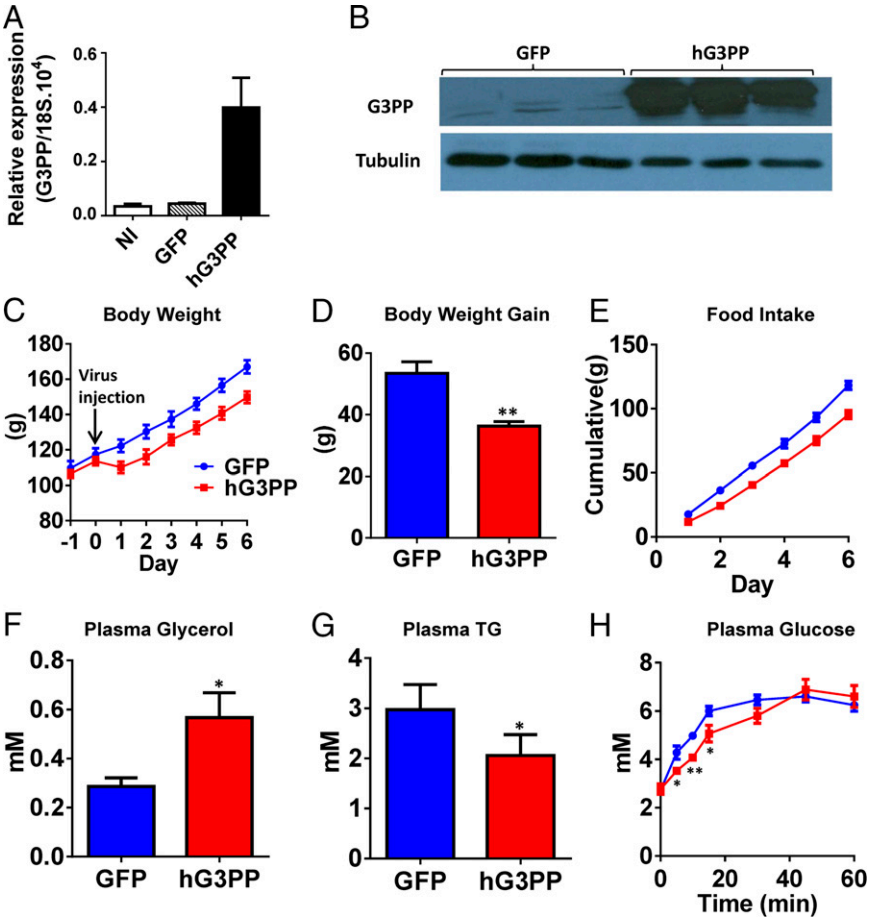

Fig. 6. In vivo study of the effect of hG3PP overexpression. Rats were injected with adenovirus expressing hG3PP ($n = 6$) or GFP ($n = 5$), and, on day 7, a glycerol load test was performed. Expression of hG3PP in liver was assessed and plasma glycerol and TG levels were measured before glycerol load (mean ± SEM; $*P < 0.05$, $**P < 0.01$, and $***P < 0.001$). (*A*) hG3Pase mRNA and (*B*) hG3PP protein levels (representative Western blots from three separate rats). (*C*) BW and (*D*) net BW gain in 7 d after adenoviral administration. (*E*) Cumulative food intake. (*F*) Plasma glycerol and (*G*) TG levels on day 7 after virus injection in 12 h fasted rats before glycerol load. (*H*) Glycerol load test in rat expressing hG3PP or control GFP to assess glycerol-derived glucose production. Blood was collected at indicated times following gavage of glycerol.

Materials and Methods

Animals. All procedures were approved by the institutional committee for the protection of animals (Comité Instituitionnel de Protection des Animaux du Centre Hospitalier de l'Université de Montréal). Five-week-old male C57BL/6N mice and Wistar rats (85–250 g) were housed on a 12-h light/dark cycle with free access to water and standard diet (15% fat by energy). Mice were fed with chow or HFD (60% calories from fat) for 8 wk. G3PP expression was evaluated in chow-fed, HFD-fed, and overnight-fasted mice.

Islet and Hepatocyte Isolation. Pancreatic islets were isolated from rats and mice (38). Isolated islets were cultured overnight at 37 °C in complete RPMI 1640 medium. Hepatocytes were isolated from rats by in situ collagenase perfusion and were seeded in DMEM complete medium.

Insulin Secretion. Insulin secretion in INS832/13 cells (39) and isolated islet cells was measured in static incubations (38). Details are given in *SI Materials and Methods*.

Overexpression and RNAi Knockdown of G3PP. pCMV-based plasmids expressing human G3PP and GFP were used. After transfection using Lipofectamine, INS832/13 cells were cultured for 48 h in 96-well, 12-well, or 6-well plates. siRNAs against G3PP and two scrambled siRNAs were introduced into INS832/13 cells by RNAiMAX (40). Transfected cells were used for Western blotting and measurements of insulin secretion, caspase activity, glycerol and FFA release, O_2 consumption, and fatty acid oxidation and esterification.

Quantitative Real-Time PCR. Total RNA was extracted from INS832/13 cells, islet cells, and rodent tissues, and first-strand cDNA was synthesized from 2 μg of total RNA. Quantitative real-time PCR (RT-qPCR) was performed, and the products were quantified by using the FastStart DNA Master PLUS SYBR green kit (Roche Diagnostics). Expression levels were normalized for the 18S or cyclophilin mRNA transcript.

FFAs and Glycerol Release. For FFA determinations, rat islet cells were preincubated for 1 h in Krebs Ringer buffer-Hepes (KRBH) containing 2 mM glutamine and 4 mM glucose and then for 2 h at 4 mM, 10 mM, 16 mM, and 25 mM glucose. The low and high glucose concentrations were 2 mM and 10 mM for INS832/13 cells with 2 mM glutamine present. Incubations were done without and with the panlipase inhibitor orlistat. FFA released into the medium was extracted by a modified Dole-Meinertz procedure and quantified by reverse-phase HPLC (40). Glycerol release was determined by a radiometric glycerol assay using [γ-^{32}P]ATP and glycerokinase.

Plasma Chemistry. TGs and glycerol were measured by using a colorimetric assay kit (Sigma), and LDL and HDL by using a kit (L-Type LDL-C; Wako).

Fatty Acid Esterification and Oxidation. Fatty acid esterification and oxidation in the transfected INS832/13 cells and infected hepatocytes were measured at low and high glucose levels as indicated in figure legends.

Glucotoxicity and Glucolipotoxicity. The effect of overexpression or knockdown of G3PP in INS832/13 cells on caspase-3 activity was assessed at 5 mM or 20 mM glucose with or without 0.3 mM palmitate.

Oxygen Consumption and Mitochondrial Function. Respiration measurements in vitro were made in a XF24 respirometer (Seahorse Bioscience) using transfected INS832/13 cells and isolated rat islets after infection with adeno- or lentivirus constructs. After basal respiration measurement for 20 min, glucose levels were elevated to 10 mM (INS cells) or 16 mM (islets). After incubations for 20 min or 1 h (INS and islet cells, respectively), oligomycin, carbonyl cyanide-4-(trifluoromethoxy)phenylhydrazone (FCCP), and antimycin/rotenone were added by three successive injections to assess uncoupled respiration, maximal respiration, and nonmitochondrial respiration, respectively.

Gluconeogenesis and Glycolysis in Hepatocytes. For gluconeogenesis determination, after infection with adeno- or lentiviral constructs, hepatocytes were starved in DMEM without glucose for 2 h, followed by incubation in glucose-free DMEM (pH 7.4) without phenol red, supplemented with 10 mM glycerol or 20 mM sodium lactate plus 2 mM sodium pyruvate, 2 mM L-glutamine, and 15 mM Hepes for 2 h. After incubation, the medium was processed for glucose measurement. Glycolysis was assessed by lactate content and lactate release measurement, as lactate is considered a reliable index of steady-state glycolysis in isolated hepatocytes in culture (41).

Adenovirus and Lentivirus Infection of Islet Cells and Hepatocytes. Islet cells and hepatocytes were infected with recombinant adenovirus (multiplicity of infection of 100) expressing GFP alone (control) or human G3PP (Vector Biolabs), both under CMV promoter control, to overexpress these proteins. To knock down endogenous G3PP, we used rat G3PP-shRNA lentivirus (multiplicity of infection of 5), with a GFP-shRNA lentivirus as control (abm). Experiments were performed 48 h after infection.

G3PP-Adenovirus Administration to Rats. Male rats (85–100 g) were housed in individual cages and given free access to standard diet. Rats received a single injection by tail vein of adenovirus (5.5×10^{10} viral particles per milliliter per 100 g BW) carrying the genes of human G3PP (Adv-hG3PP) or GFP (Adv-GFP) as control. Rats were given FK506 (0.2 mg/kg BW) on the day before and on the day of the virus administration to minimize the immune response. Food consumption and BW were monitored daily for 7 d following virus injection. Then, food was withdrawn for 12 h from the rats and a glycerol load test was performed. Rats were killed and blood and different tissues were collected for analyses.

Oral Glycerol Load Test. Rats injected with Adv-G3PP or Adv-GFP were fed a chow diet for 1 wk and, on the seventh day, food was withdrawn for 12 h. Then, 87% (wt/vol) glycerol (5 mg/g BW) was administered orally. Blood was collected from the tail vein before and at 5 min, 10 min, 20 min, 30 min, 50 min, and 60 min after glycerol load, and blood glucose was measured by using a glucometer.

PGP/G3PP Protein Expression and Activity in Vitro. Purified recombinant murine PGP/G3PP (18) was assayed by using EnzChek Phosphate Assay Kit (Invitrogen/Molecular Probes). The reaction mix in a volume of 100 μL, containing 50 mM triethanolamine·HCl, 200 mM NaCl, 5 mM $MgCl_2$ (pH 7.5), and indicated concentrations of Gro3P, was preincubated for 10 min at room temperature. The reaction at 37 °C was started by the addition of 1 μg purified PGP/G3PP, and phosphatase activity was then monitored by measuring absorbance at 360 nm in a microplate reader (Spectramax Plus 384; Molecular Devices) and corrected for background absorbance. Human PGP/G3PP in extracts of overexpressing 293T cells (10 μg cell extract protein) or control INS832/13 cells (30 μg cell extract protein) was assayed by using a Phosphate Colorimetric Assay Kit (BioVision). The reaction mix (final volume, 200 μL) containing 50 mM triethanolamine·HCl, 200 mM NaCl, 5 mM $MgCl_2$ (pH 7.5), indicated concentrations of Gro3P, 2-PG, and glucose-6-phosphate was preincubated for 30 min at 37 °C with shaking, and the reaction was started by the addition of G3PP overexpressed or control extracts and continued for 10 min. Phosphatase activity was monitored by measuring the absorbance at 650 nm on a microplate reader (Greiner Bio-one). To derive K_M and K_{cat} values, the data were fit by nonlinear regression to the Michaelis-Menten equation by using GraphPad Prism.

Targeted Metabolomics in Rat Hepatocytes. After infection with adeno- or lentiviral constructs, primary hepatocytes were starved without glucose in DMEM for 2 h, followed by incubation in glucose-free DMEM (pH 7.4) without phenol red, supplemented with 5 mM or 25 mM glucose for 2 h. After incubation, medium was removed and metabolism rapidly quenched by transferring culture plates in liquid nitrogen. Metabolites were extracted as described previously (31) with the following modifications. Cells were scraped on ice and collected in 675 μL ice-cold extraction buffer [80% (vol/vol) methanol, 13.7 mM ammonium acetate, pH 9.0, with 10 μM ($^{13}C_{10}$,$^{15}N_5$)-adenosine-5′-monophosphate lithium salt as internal standard], transferred into polypropylene (PP) tubes, and sonicated in a cup-horn sonicator at 150 W for 2 min (cycles of 10 s on, 10 s off) in an ethanol/ice bath. Cell extracts were centrifuged at 4 °C for 10 min at 25,830 × *g*, and supernatants were collected in ice-cold 2-mL PP tubes, to which 250 μL water was added. Polar metabolites were extracted with 1,080 μL of chloroform:heptane (3:1 vol/vol) by 2 × 10 s vortex followed by 10-min incubation on ice and 15-min centrifugation at 4 °C, 12,500 × *g*. From the upper phase, 600 μL was collected without carrying out any interface material and transferred into new cold 2-mL PP tubes. These tubes were centrifuged again, and 400 μL supernatant were collected into cold 1.5-mL PP tubes. Samples were frozen in liquid nitrogen and dried in two steps—first, in a SpeedVac Concentrator for ∼2 h (maximal vacuum, no heat; Savant) at 4 °C to remove methanol; and second, by lyophilization for 90 min (Labconco FreeZone) —and then stored at −80 °C until used. Samples were reconstituted in 14 μL of Milli-Q water, and injections of 3 μL were performed in duplicate on an electrospray ionization LC-MS/MS system composed of an Agilent 1200 SL device (for LC) and a triple-quadrupole mass spectrometer (4000Q TRAP MS/MS; Sciex). Samples were separated by gradient elution of 12 min on a Poroshell 120 EC-C18, 2.1 × 75-mm, 2.7-μm column (Agilent Technologies) using mobile phase consisting of an aqueous

solvent A (10 mM tributylamine, 15 mM acetic acid, pH 5.2) and an organic solvent B [95% (vol/vol) acetonitrile in water, 0.1% formic acid], at a flow rate of 0.75 mL/min and column oven temperature of 40 °C. The MS was operated in negative electrospray ionization mode using a turbo ion spray source. Transitions used were described previously (31), with additional selected ion monitoring at mass/charge ratios of 154.75/78.79, for 2-PG and glycolate. Quantification was performed as described before (31).

Statistical Analysis. Values are expressed as means ± SEM. Statistical significance was calculated with one-way or two-way ANOVA with Bonferroni or Dunnett post hoc testing for multiple comparisons or the Student *t* test as indicated. A P value of <0.05 was considered significant.

ACKNOWLEDGMENTS. The authors thank the Metabolomics Core Facility of the Centre de Recherche du Centre Hospitalier de l'Université de Montréal for performing the metabolite determinations. This study was supported by grants from Canadian Institutes of Health Research (to M.P. and S.R.M.M.), NIH Grant R01-DK19514 (to M.P. and Neil Ruderman, Boston University), Deutsche Forschungsgemeinschaft Grant SFB688 (to A.G.), Forschungszentrum Grant FZ82 (to A.G.), and a fellowship from Fond de Recherche Santé Québec (to Y.M.). M.P. holds the Canada Research Chair in Diabetes and Metabolism.

1. Nye CK, Hanson RW, Kalhan SC (2008) Glyceroneogenesis is the dominant pathway for triglyceride glycerol synthesis in vivo in the rat. *J Biol Chem* 283(41):27565–27574.
2. Zechner R, et al. (2012) FAT SIGNALS–lipases and lipolysis in lipid metabolism and signaling. *Cell Metab* 15(3):279–291.
3. Prentki M, Madiraju SR (2008) Glycerolipid metabolism and signaling in health and disease. *Endocr Rev* 29(6):647–676.
4. Prentki M, Madiraju SR (2012) Glycerolipid/free fatty acid cycle and islet β-cell function in health, obesity and diabetes. *Mol Cell Endocrinol* 353(1-2):88–100.
5. Peyot ML, et al. (2010) Beta-cell failure in diet-induced obese mice stratified according to body weight gain: Secretory dysfunction and altered islet lipid metabolism without steatosis or reduced beta-cell mass. *Diabetes* 59(9):2178–2187.
6. Green CD, Jump DB, Olson LK (2009) Elevated insulin secretion from liver X receptor-activated pancreatic beta-cells involves increased de novo lipid synthesis and triacylglyceride turnover. *Endocrinology* 150(6):2637–2645.
7. Zhang C, Klett EL, Coleman RA (2013) Lipid signals and insulin resistance. *Clin Lipidol* 8(6):659–667.
8. Delghingaro-Augusto V, et al. (2009) Islet beta cell failure in the 60% pancreatectomised obese hyperlipidaemic Zucker fatty rat: Severe dysfunction with altered glycerolipid metabolism without steatosis or a falling beta cell mass. *Diabetologia* 52(6):1122–1132.
9. Nolan CJ, et al. (2006) Beta cell compensation for insulin resistance in Zucker fatty rats: Increased lipolysis and fatty acid signalling. *Diabetologia* 49(9):2120–2130.
10. Wilfling F, Haas JT, Walther TC, Farese RV, Jr (2014) Lipid droplet biogenesis. *Curr Opin Cell Biol* 29:39–45.
11. Ditlecadet D, Driedzic WR (2013) Glycerol-3-phosphatase and not lipid recycling is the primary pathway in the accumulation of high concentrations of glycerol in rainbow smelt (Osmerus mordax). *Am J Physiol Regul Integr Comp Physiol* 304(4):R304–R312.
12. Previs SF, et al. (1995) Limitations of the mass isotopomer distribution analysis of glucose to study gluconeogenesis. Substrate cycling between glycerol and triose phosphates in liver. *J Biol Chem* 270(34):19806–19815.
13. Larrouy-Maumus G, et al. (2013) Discovery of a glycerol 3-phosphate phosphatase reveals glycerophospholipid polar head recycling in Mycobacterium tuberculosis. *Proc Natl Acad Sci USA* 110(28):11320–11325.
14. Fan J, Whiteway M, Shen SH (2005) Disruption of a gene encoding glycerol 3-phosphatase from Candida albicans impairs intracellular glycerol accumulation-mediated salt-tolerance. *FEMS Microbiol Lett* 245(1):107–116.
15. Norbeck J, Påhlman AK, Akhtar N, Blomberg A, Adler L (1996) Purification and characterization of two isoenzymes of DL-glycerol-3-phosphatase from Saccharomyces cerevisiae. Identification of the corresponding GPP1 and GPP2 genes and evidence for osmotic regulation of Gpp2p expression by the osmosensing mitogen-activated protein kinase signal transduction pathway. *J Biol Chem* 271(23):13875–13881.
16. Caparrós-Martín JA, McCarthy-Suárez I, Culiáñez-Macià FA (2014) The kinetic analysis of the substrate specificity of motif 5 in a HAD hydrolase-type phosphosugar phosphatase of Arabidopsis thaliana. *Planta* 240(3):479–487.
17. Rose ZB (1981) Phosphoglycolate phosphatase from human red blood cells. *Arch Biochem Biophys* 208(2):602–609.
18. Seifried A, et al. (2014) Evolutionary and structural analyses of mammalian haloacid dehalogenase-type phosphatases AUM and chronophin provide insight into the basis of their different substrate specificities. *J Biol Chem* 289(6):3416–3431.
19. Lahiri SD, Zhang G, Dunaway-Mariano D, Allen KN (2006) Diversification of function in the haloacid dehalogenase enzyme superfamily: The role of the cap domain in hydrolytic phosphorus carbon bond cleavage. *Bioorg Chem* 34(6):394–409.
20. Seifried A, Schultz J, Gohla A (2013) Human HAD phosphatases: structure, mechanism, and roles in health and disease. *FEBS J* 280(2):549–571.
21. Prentki M, Matschinsky FM, Madiraju SR (2013) Metabolic signaling in fuel-induced insulin secretion. *Cell Metab* 18(2):162–185.
22. Prentki M, Joly E, El-Assaad W, Roduit R (2002) Malonyl-CoA signaling, lipid partitioning, and glucolipotoxicity: Role in beta-cell adaptation and failure in the etiology of diabetes. *Diabetes* 51(suppl 3):S405–S413.
23. El-Assaad W, et al. (2010) Glucolipotoxicity alters lipid partitioning and causes mitochondrial dysfunction, cholesterol, and ceramide deposition and reactive oxygen species production in INS832/13 ss-cells. *Endocrinology* 151(7):3061–3073.
24. Christoffersen C, et al. (2003) Cardiac lipid accumulation associated with diastolic dysfunction in obese mice. *Endocrinology* 144(8):3483–3490.
25. Vaughan M (1962) The production and release of glycerol by adipose tissue incubated in vitro. *J Biol Chem* 237:3354–3358.
26. Wendel AA, Cooper DE, Ilkayeva OR, Muoio DM, Coleman RA (2013) Glycerol-3-phosphate acyltransferase (GPAT)-1, but not GPAT4, incorporates newly synthesized fatty acids into triacylglycerol and diminishes fatty acid oxidation. *J Biol Chem* 288(38):27299–27306.
27. Frayn KN (2010) Fat as a fuel: Emerging understanding of the adipose tissue-skeletal muscle axis. *Acta Physiol (Oxf)* 199(4):509–518.
28. Thai M, et al. (2014) Adenovirus E4ORF1-induced MYC activation promotes host cell anabolic glucose metabolism and virus replication. *Cell Metab* 19(4):694–701.
29. Bardell D (1977) Glucose uptake and lactic acid production of adenovirus type 5-infected HEp-2 cells cultured under exponential growth and stationary phase conditions. *Microbios* 20(81-82):139–144.
30. Berry MN, Barritt GJ, Edwards AM (1991) *Isolated Hepatocytes. Preparation, Properties and Applications* (Elsevier, Amsterdam).
31. Guay C, et al. (2013) A role for cytosolic isocitrate dehydrogenase as a negative regulator of glucose signaling for insulin secretion in pancreatic ß-cells. *PLoS One* 8(10):e77097.
32. Chen B, et al. (2007) GC/MS methods to quantify the 2-deoxypentos-4-ulose and 3′-phosphoglycolate pathways of 4′ oxidation of 2-deoxyribose in DNA: Application to DNA damage produced by gamma radiation and bleomycin. *Chem Res Toxicol* 20(11):1701–1708.
33. Knight J, Hinsdale M, Holmes R (2012) Glycolate and 2-phosphoglycolate content of tissues measured by ion chromatography coupled to mass spectrometry. *Anal Biochem* 421(1):121–124.
34. de Groot MJ, de Jong YF, Coumans WA, van der Vusse GJ (1994) The hydrolysis of glycerol-3-phosphate into glycerol in cardiac tissue: Possible consequences for the validity of glycerol release as a measure of lipolysis. *Pflugers Arch* 427(1-2):96–101.
35. Ditlecadet D, Driedzic WR (2014) Glycerol synthesis in freeze-resistant rainbow smelt: Towards the characterization of a key enzyme glycerol-3-phosphatase. *Fish Physiol Biochem* 40(1):257–266.
36. Moriyama M, et al. (2015) Mechanism for increased hepatic glycerol synthesis in the citrin/mitochondrial glycerol-3-phosphate dehydrogenase double-knockout mouse: Urine glycerol and glycerol 3-phosphate as potential diagnostic markers of human citrin deficiency. *Biochim Biophys Acta* 1852(9):1787–1795.
37. Madiraju AK, et al. (2014) Metformin suppresses gluconeogenesis by inhibiting mitochondrial glycerophosphate dehydrogenase. *Nature* 510(7506):542–546.
38. Peyot ML, et al. (2009) Adipose triglyceride lipase is implicated in fuel- and non-fuel-stimulated insulin secretion. *J Biol Chem* 284(25):16848–16859.
39. Hohmeier HE, et al. (2000) Isolation of INS-1-derived cell lines with robust ATP-sensitive K+ channel-dependent and -independent glucose-stimulated insulin secretion. *Diabetes* 49(3):424–430.
40. Zhao S, et al. (2014) α/β-Hydrolase domain-6-accessible monoacylglycerol controls glucose-stimulated insulin secretion. *Cell Metab* 19(6):993–1007.
41. Phillips JW, Clark DG, Henly DC, Berry MN (1995) The contribution of glucose cycling to the maintenance of steady-state levels of lactate by hepatocytes during glycolysis and gluconeogenesis. *Eur J Biochem* 227(1-2):352–358.
42. Merlen G, et al. (2014) AMPKα1 controls hepatocyte proliferation independently of energy balance by regulating Cyclin A2 expression. *J Hepatol* 60(1):152–159.
43. Püttmann M, Krug H, von Ochsenstein E, Kattermann R (1993) Fast HPLC determination of serum free fatty acids in the picomole range. *Clin Chem* 39(5):825–832.
44. Mehta A, Oeser AM, Carlson MG (1998) Rapid quantitation of free fatty acids in human plasma by high-performance liquid chromatography. *J Chromatogr B Biomed Sci Appl* 719(1-2):9–23.
45. Bradley DC, Kaslow HR (1989) Radiometric assays for glycerol, glucose, and glycogen. *Anal Biochem* 180(1):11–16.
46. Friedewald WT, Levy RI, Fredrickson DS (1972) Estimation of the concentration of low-density lipoprotein cholesterol in plasma, without use of the preparative ultracentrifuge. *Clin Chem* 18(6):499–502.
47. Segall L, et al. (1999) Lipid rather than glucose metabolism is implicated in altered insulin secretion caused by oleate in INS-1 cells. *Am J Physiol* 277(3 pt 1):E521–E528.
48. Saddik M, Lopaschuk GD (1991) Myocardial triglyceride turnover and contribution to energy substrate utilization in isolated working rat hearts. *J Biol Chem* 266(13):8162–8170.
49. Lamontagne J, et al. (2009) Pioglitazone acutely reduces insulin secretion and causes metabolic deceleration of the pancreatic beta-cell at submaximal glucose concentrations. *Endocrinology* 150(8):3465–3474.
50. Qiang L, et al. (2012) Brown remodeling of white adipose tissue by SirT1-dependent deacetylation of Pparγ. *Cell* 150(3):620–632.
51. Maughan RJ (1982) A simple, rapid method for the determination of glucose, lactate, pyruvate, alanine, 3-hydroxybutyrate and acetoacetate on a single 20-mul blood sample. *Clin Chim Acta* 122(2):231–240.